Inductively Coupled Planar TX Coils: Analysis of B_1^+ Efficiency and SAR Performance

Johanna Schöpfer[1,2], Klaus Huber[2], Stephan Biber[3], Markus Vester[3], Sebastian Martius[2], and Martin Vossiek[1]

[1]*LHFT, University of Erlangen-Nuremberg, Erlangen, Germany,* [2]*Siemens AG, Corporate Technology, Erlangen, Germany,* [3]*Siemens AG, Healthcare, Erlangen, Germany*

Introduction: For the excitation of the radio frequency transmit field in today's clinical magnetic resonance imaging, the full-body birdcage is used almost exclusively. Imaging time can be limited by local and global SAR values, especially in 3T MRI. This is of particular interest when imaging patients with metal implants, where very high B_1^+ fields are required to reduce artifacts [1]. Due to their inherently reduced power requirements, local transmit coils are well suited for this special application. Another approach to get a more focused and strong transmit field are inductively coupled coils [2]. When imaging body parts not accessible with volume coil designs (e.g. spine, shoulder), planar antenna structures have to be used. The purpose of this study is to evaluate potential benefits of using inductively coupled resonant planar loops during transmission by comparing the transmit characteristics of the body coil with and without additional resonant loops in terms of maximum available B_1^+ field and SAR.

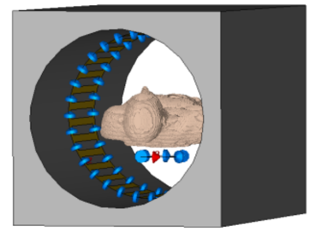

Figure 1: *Simulation setup*

Methods: A full-body birdcage coil was modeled in Microwave Studio (CST, Darmstadt, Germany) and tuned to 123.2 MHz using lumped capacitors in the 3D model. A human-body model ("Duke" [3]) was inserted to achieve a realistic local-SAR estimation (Figure 1). In a second step, a resonant circular loop was added to the original simulation setup. In order to evaluate the effect of the load, the distance between the loop and the human body was varied between 3 cm and 1 cm. These distances would allow for a future integration of the resonant circular loop in the patient table without major changes. For a fair evaluation, the transmit fields and global/local SAR were calculated, exported and scaled to a defined reference B_1^+ field using MATLAB. To further verify the concept and the simulation, phantom measurements on a Siemens MAGNETOM Skyra 3T were carried out. The prototype resonant loop with a diameter of 20 cm was manufactured with adhesive copper tape on an FR4 substrate and was tuned to resonance frequency by the use of high-voltage ceramic capacitors. For the MRI experiment it was attached to a Body 18 RX coil and detuned during RX with an additional series pin diode, which slightly decreases the unloaded Q of the coil to a still sufficiently high value of 400.

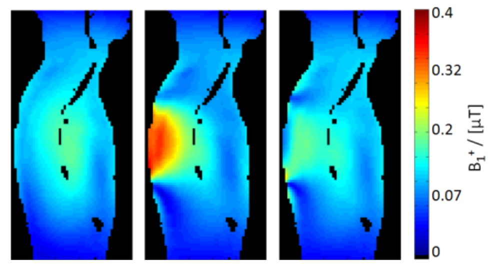

Figure 2: *B_1^+ field distribution calculated for $P_{in} = 1$; Left: Body coil, Middle: Loop placed in 3 cm distance, Right: Loop placed in 1 cm distance*

Results: The transmit field distributions inside the human body model for three simulations with and without a resonant circular loop (diameter 20 cm) are shown in Figure 2. The transmit field is clearly enhanced in the ROI (human C-spine) due to the presence of the resonant loop. The respective field strength depends significantly on the distance between the loop and the body. For short distances, the loaded Q factor gets smaller and thus less current is induced, which in turn leads to less field focusing. The maximum current is reduced by approx. 30 % between the setups with distances of 3 cm compared to 1 cm, whereas the s-parameters of the body coil remain constant. In Table 1, the required power and the corresponding change in global/local SAR, calculated for an average reference B_1^+ field of 11.75 µT in the defined ROI (human spine), are summarized for different antenna setups. For a loop distance of 3 cm, only 25 % of the power is required compared to the standard body coil which corresponds to a 75 % saving of global SAR. However, local SAR is only reduced slightly in the 3 cm setup and even increased for the two setups in which the loop is placed closer to the body. The transmit field homogeneity in the ROI is similar to that of the body coil for each of the three distances. The experimental verification was done on a Siemens MAGNETOM Skyra with native elliptic polarized excitation. Flip angle maps for various coil setups and transmit powers were evaluated using standard service routines. The experimental data are in good agreement with the simulation results (see Figure 3). In Figure 4, the experimental setup and GRE images with and without the resonant loop are shown. In this particular case, the transmitter adjustment voltage with the resonant loop in place is 178 V compared to 280 V for the natural body coil excitation, which means a 60 % power reduction due to the resonant loop.

	Power requirements	local SAR (10g)	global SAR
Loop in distance 3cm	25%	93%	25%
Loop in distance 2cm	44%	133%	42%
Loop in distance 1cm	63%	151%	61%

Table 1: *Increase/decrease of power consumption & local and global SAR for a reference $B_1^+ = 11.75$ µT in ROI. All results are relative to an excitation with the standard body coil.*

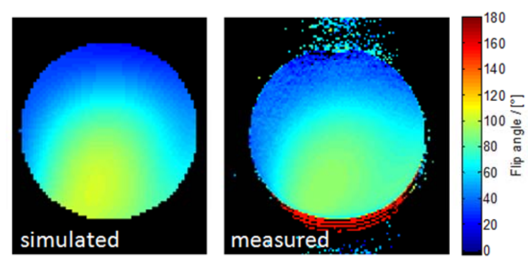

Figure 3: *Simulated and measured flip angle map*

Conclusion: The study highlights the benefits of inductively coupled planar loop coils in order to focus the transmit field in a defined ROI. For a properly chosen distance between loop and human body, the required power can be reduced by a factor of four, without compromising B_1^+ homogeneity significantly in the ROI.

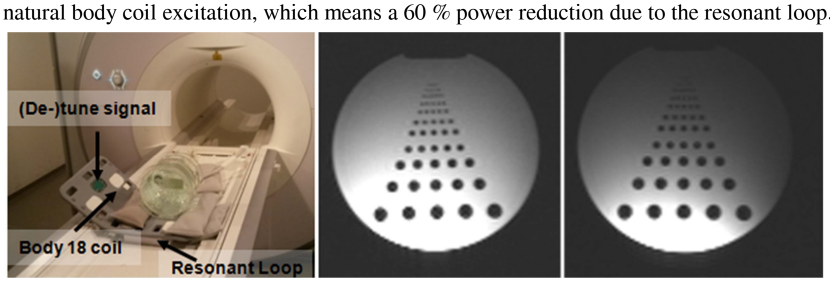

Figure 4: *Measurements on MRI scanner. Left: Prototype measurement setup (resonant loop placed below Body 18 coil), Middle: GRE, Body coil excitation $U_{ref} = 280$ V, Right: GRE, Body coil and resonant loop, $U_{ref} = 178$ V*

References:[1] Bachschmidt et.al; Knee implant imaging at 3 Tesla using high-bandwidth radiofrequency pulses, JMRI (2014) [2] Wang et.al; Inductive Coupled Local TX Coil Design, Proc. Intl. Soc. Mag. Reson. Med 18 (2010) [3] Christ, et. al; Development of surface based anatomical Models of Two Adults and Two Children for Dosimetric Simulations: Phys. Med. Biol. Vol. 55 Issue 2; (2010)